Investigation of lower hybrid current drive during H-mode in EAST tokamak*

Li Miao-Hui(李妙辉)†, Ding Bo-Jiang(丁伯江), Kong Er-Hua(孔二华), Zhang Lei(张 磊), Zhang Xin-Jun(张新军), Qian Jin-Ping(钱金平), Yan Ning(颜 宁), Han Xiao-Feng(韩效锋), Shan Jia-Fang(单家方), Liu Fu-Kun(刘甫坤), Wang Mao(王 茂), Xu Han-Dong(徐昂东), and Wan Bao-Nian(万宝年)

Institute of Plasma Physics, Chinese Academy of Sciences, Hefei 230031, *China*

(Received 20 March 2011; revised manuscript received 15 June 2011)

H-mode discharges with lower hybrid current drive (LHCD) alone are achieved in EAST divertor plasma over a wide parameter range. These H-mode discharges are characterized by a sudden drop in D_α emission and a spontaneous rise in main plasma density. Good lower hybrid (LH) coupling during H-mode is obtained by putting the plasma close to the antenna and by injecting D_2 gas from a pipe near the grill mouse. The analysis of lower hybrid current drive properties shows that the LH deposition profile shifts off axis during H-mode, and current drive (CD) efficiency decreases due to the increase in density. Modeling results of H-mode discharges with a general ray tracing code GENRAY are reported.

Keywords: H-mode, edge localized mode, lower hybrid current drive

PACS: 52.50.Sw, 52.65.Ff, 52.40.Db **DOI:** 10.1088/1674-1056/20/12/125202

1. Introduction

The H-mode is a high confinement mode of toroidal plasmas, which was first discovered in ASDEX 28 years ago by Wagner *et al.*[1] Later the H-mode was also obtained in PDX divertor discharges with neutral beam injection (NBI),[2] in JET with ion cyclotron resonance heating (ICRH),[3] and even in COMPASS-D with Ohmic heating alone.[4] The directly observable signatures of H-mode characteristics are an evident drop of D_α/H_α emission in the divertor, which indicates how much power flows into the divertor chamber across the separatrix, a steep pressure gradient at the plasma edge (usually called pedestal), and a doubled energy confinement time compared with the normal L-mode scenario. Finally, the so-called edge localized modes (ELMs)[5] are often observed in this regime due to the MHD instability. The necessary requirement for L–H transition is that the heating power should exceed the power threshold, which varies with density, magnetic field, and machine size. There is a general consensus that the transition from L- to H-mode is caused by a reduction of anomalous transport at the plasma edge (i.e. the establishment of the transport barrier). Some other theories and experiments show that this transition is concerned with the decorrelation of turbulent eddies by radially sheared $\boldsymbol{E}\times\boldsymbol{B}$ flow residing at the plasma edge.[6] Although the understanding of the physics behind the H-mode is not very clear, its value is unquestioned. Just as the saying goes, H-mode is what makes the goals of fusion achievable. Moreover, the ITER design is based on the ELMy H-mode to achieve its $Q = 10$ mission. In this paper, we report on the first observation of H-mode in EAST divertor plasma with lower hybrid current drive (LHCD) alone and some properties of lower hybrid (LH) coupling and current drive (CD) efficiency during H-mode.

2. Experimental setup

EAST is a fully superconducting tokamak with a D-shaped vacuum vessel (major radius $R = 1.82$ m, minor radius $a = 0.45$ m), allowing discharges in single null divertor (SND) and double null divertor (DND) configurations. The LHCD, as a main CD

*Project supported by the National Natural Science Foundation of China (Grant Nos. 10875149 and 10805057) and the National Magnetic Confinement Fusion Science Program of China (Grant No. 2010GB105004).

†Corresponding author. E-mail: mhli@ipp.ac.cn

© 2011 Chinese Physical Society and IOP Publishing Ltd

and auxiliary heating system for EAST, operates at a frequency $f = 2.45$ GHz and consists of 20 multi-junction waveguides.[7] At present, the maximum output power is about 1.4 MW. Due to the magnetic flux limitation of the transformer, the longest duration of H-mode discharges in this campaign is 6.4 s (Shot No.: 36609), in a combination of LHCD and ICRH. With a favourable ∇B drift direction, ELMy H-mode plasmas with LH alone have been obtained reproducibly over a wide parameter range: 0.4 MA $\leq I_{\rm p} \leq$ 0.8 MA, 1.3 T $\leq B_{\rm t} \leq$ 2 T, 2×10^{19} m^{-3} $\leq n_{\rm e_av} \leq 3.5\times10^{19}$ m^{-3}, single SND and DND configurations.

3. Results and discussion

Figure 1 displays some typical traces of an H-mode discharge where $P_{\rm LH} = 0.75$ MW power was injected with the parallel refraction index $N_{\|0} = 2.1$ (note that, in consideration of the power loss along the transmission line and due to the wave scattering by density fluctuation at the plasma edge, the absorbed power by resonant electrons $P_{\rm LH} = \alpha P_{\rm RF}$, where $P_{\rm RF}$ is the launched power and α is assumed to be 0.8). In order to reduce both the impurity recycling and the hydrogen recycling, the lithium powder was dropped at $t = 0.5$ s and lasted 1 s. Additionally, the plasma shape was converted into divertor configuration (triangularity $\delta \sim 0.5$ and elongation $\kappa \sim 1.7$) as early as at 0.8 s, with the purpose of reducing plasma radiation. The gap, which is related to the duration of the H-mode,[8] between the lost closed flux surface (LCFS) and the outer first wall was about 6 cm. The plasma was developed from deuterium gas with the central magnetic field $B_{\rm t} \sim 1.57$ T, and the plasma current was 0.5 MA, resulting in $q_{95} \sim 3.9$. The L–H transition was triggered at 3.0 s, featuring a sharp drop of D_α emission in the divertor chamber, an apparent increase in both plasma stored energy ($\Delta W_{\rm dia} \sim 35$ kJ) and line-averaged electron density ($n_{\rm e_av}$), and the H-mode plasma lasted 0.9 s. After the L-H transition, the discharge entered into a short ($\sim$ 0.1 s) quiescent H phase, during which the plasma stored energy and line-averaged density increased rapidly, owing to the improvement of global confinement, and then the large ELMs burst with a frequency of about 0.25 kHz at a nearly constant density of 3.0×10^{19} m^{-3}, twice as large as that in L-mode. The large ELMs were accompanied by the radiation of carbon impurity in the divertor (see the curve in the bottom box of Fig. 1), which behaved almost in the same way as deuterium. The energy confinement time evaluated from $\tau_{\rm E} = W_{\rm dia}/(P_{\rm OH} + P_{\rm LH} - {\rm d}W_{\rm dia}/{\rm d}t)$ by using diamagnetic loop measurements was about 78 ms in the H phase and the confinement enhancement factor defined as $HH = \tau_{\rm E}/\tau_{\rm E}^{\rm IPB98,y2}$ was equivalent to 0.9, where the so-called IPB98 (y, 2) scaling for the ELMy H-mode was expressed as[9]

$$\tau_{\rm E}^{\rm IPB98,y2} = 0.0562 I_{\rm P}^{0.93} B_{\rm T}^{0.15} n_{19}^{0.41} P^{-0.69} \times R^{1.97} \varepsilon^{0.58} \kappa^{0.78} M^{0.19}, \quad (1)$$

where $\tau_{\rm E}$, $I_{\rm P}$, $B_{\rm T}$, n_{19}, P, R are respectively in units of s, MA, T, 10^{19} m^{-3}, MW, m, $\varepsilon = a/R$ is inverse aspect ratio, and M is ion mass number.

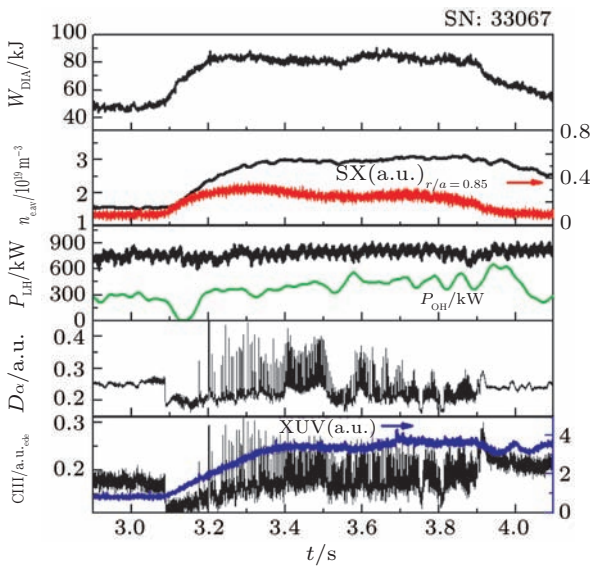


Fig. 1. (colour online) A typical ELMy H-mode discharge with LH; $W_{\rm DIA}$ denotes the plasma stored energy, $n_{\rm e_av}$ the line averaged density, SX the soft-X-ray signal through Be foil, $P_{\rm LH}$ the LH heating power, $P_{\rm OH}$ the Ohmic heating power, D_α the deuterium emission in the divertor, CIII the carbon radiation along chords near the edge, and XUV the radiation loss signal through the centre.

The $T_{\rm e}$ and $n_{\rm e}$ profiles measured by Thomson scattering system to an accuracy of 15% are shown in Fig. 2, from which we can see that the two shapes in H phase are both very different from these in L-mode. Firstly, the temperature profile maintains a broad shape inside the edge transport barrier (ETB) and the magnitude seems 100 eV–200 eV lower than that of L circumstance, resulting from the unfavourable radiation loss from the plasma core (see XUV signal in Fig. 1 bottom box). Unfortunately, the reasons for

so strong energy loss are not clear in this campaign and may be linked to a strong impurity accumulation or a peaked density distribution in the plasma centre. Conversely, the edge temperature is apparently higher, indicating that the edge pedestal is formed. This conclusion can also be drawn from the time evolution of soft-X-ray emission near the edge with Be foils of 25 μm in thickness as shown by the curves in the second box from the top of Fig. 1. Secondly, the electron density increases obviously during H-mode in all regions and the gradient becomes steeper near the margin. Moreover, the peakedness factor of the density profile, $n_e(0)/n_{e_av}$, changes from about 1.7 during L-mode phase to around 1.5 during smooth H-mode phase.

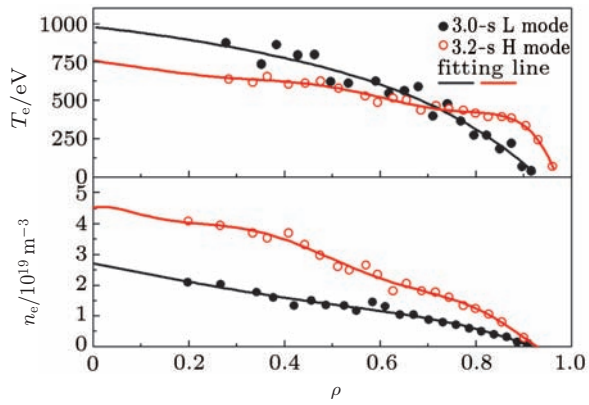


Fig. 2. (colour online) Electron temperature and density profiles determined from Thomson scattering.

One of the necessary conditions is that the auxiliary heating power should be above the threshold power P_{th} required for the L–H transition. Global scaling expression for the energy confinement time τ_E as Eq. (1) or the power threshold is powerful tool for predicting the confinement performance of burning plasmas even for the present ITER design. Although the total input power $P_{tot} = P_{LH} + P_{OH}$ is limited to the range of 0.8 MW–1.4 MW, the statistical distribution of P_{th} roughly meets the scaling law[10]

$$P_{th} = 0.042 n_{20}^{0.73} B_T^{0.74} S^{0.98} \text{ (MW)}, \qquad (2)$$

where S is the plasma surface area in m^2. This result should provide a good demonstration for ITER to achieve good confinement with the heating power close to the threshold power.

The properties of energy confinement are illustrated in Fig. 3. It is not clear that the plasma stored energy increases with the total heating power, and the presumable reason is the limitation of power range. By comparing H phase and L phase, we find that the stored energy is about 80 kJ–100 kJ during H-mode discharges, and 30 kJ–60 kJ for L-mode. Note that the circled scatter that represents the maximum stored energy of 165 kJ is calculated from a discharge with plasma current $I_p = 800$ kA ($P_{OH} = 0.56$ MW), while the majority of other data points are selected from discharges with $I_p = 500$ kA–600 kA, which indicates that Ohmic heating is a more efficient way than any radio frequency heating method.

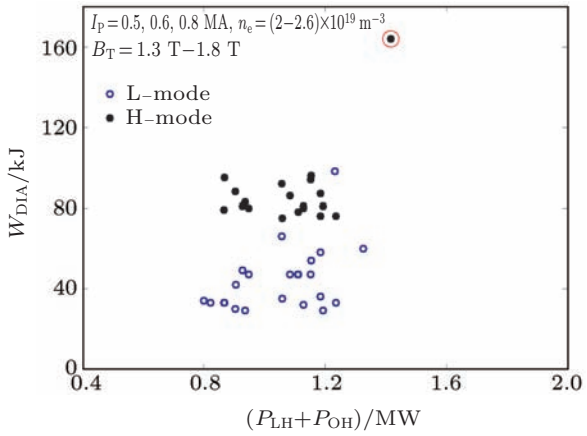


Fig. 3. (colour online) Plasma stored energy versus total input power for L-mode and H-mode.

It should be noted that the LH coupling, which may be constrained by the density in front of the launcher, is a critical issue in particular for H-mode regimes. At first the H-mode, which usually accompanies the ELMs, originates both from the steep density profile (corresponding to short density decay length) in the scrape-off layer (SOL) and from the very low density in front of the LH antenna. The cut-off density, n_{co}, below which the slow wave does not propagate, is given by $n_{co} = 0.0124 \times f^2 (10^{18}$ m$^{-3})$, and the appropriate electron density for coupling conditions is typically (2–5)×n_{co}, where f is the launched wave frequency.[11] For the LHCD system in EAST which operates at $f = 2.45$ GHz, n_{co} equals 0.074×10^{18} m^{-3}, corresponding to an optimum density of 0.32×10^{18} m^{-3}. Figure 4 shows some typical properties for two similar plasmas (an ELMy H-mode pulse and an L-mode pulse) in both edge and SOL measured by fast reciprocating Langmuir probes.[12] The H-mode data were obtained 0.3 s–0.45 s after the transition during the probe insertion. Indeed during the H phase the density profile in SOL becomes much steeped than that in L phase, and the value approximates to 0.07×10^{18} m^{-3} around the launcher, which

is much smaller than the optimum value. The electron temperature during the H phase is characterized by a large increase in the $\Delta r = 0.5$ cm–3 cm and $\Delta r = 4$ cm–6 cm regions, presumably because excessive LH power is deposited at the boundary by the strong density fluctuations, and in front of the coupler it is ~ 10 eV. Furthermore, the pedestal regime is formed as seen from the sharp pressure profile at 1 cm inside the LCFS. Secondly, the ELMs cause large unbalanced reflections, frequent trips of LHCD system and considerable reduction of the average coupled power. As a result, great efforts were made in this campaign to improve the LH coupling in the following ways: (i) controlling the distance between plasma and launcher; (ii) injecting proper gases from pipes near the LH antenna. In EAST scale tokamaks, good coupling can be obtained by moving the antenna or the plasma radially during the pulse on condition that the interaction between antenna and plasma can be neglected. Figure 5 shows a typical example of coupling improvement by putting the plasma 2 cm closer to the antenna. The averaged reflection coefficient of #33336 discharge with lower line averaged density is about 4.1%, while the coefficient of #33335 discharge reaches 5.4%, which indicates that the key to good coupling is the local density, not the bulk density, increasing around the antenna. This conclusion is in good accordance with the results obtained in Ref. [13]. In addition, the evolution of OV line signals indicates that no significant impurity is produced. The later method should be suited to tokamaks with a powerful auxiliary heating system, such as ITER, and also used to enhance the coupling during H-mode.[11] Finally, an unfavourable phenomenon of LH coupling constrained by applying simultaneous ICRH, which was installed next to the LHCD port, was observed experimentally due to the magnetic connection between the antennae. The solutions to this problem are under investigation. However, it seems that the combination of LHCD and ICRH can improve the ICRH coupling when the LH power exceeds a critical value.[14]

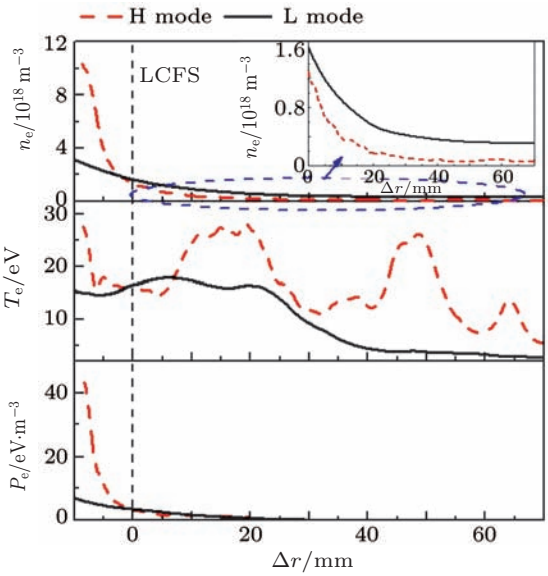


Fig. 4. (colour online) Radial profiles of electron density (n_e), temperature (T_e), and plasma pressure (P_e) against distance from the LCFS (Δr).

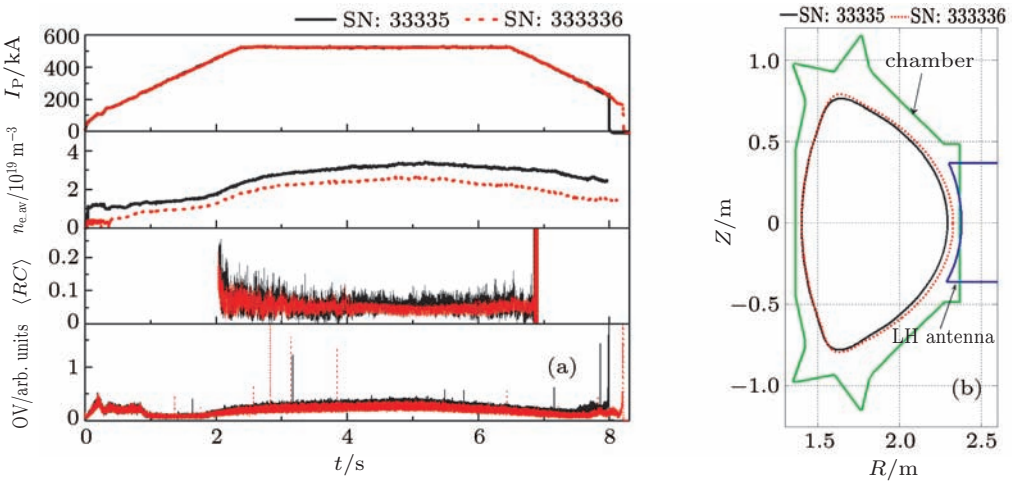


Fig. 5. (colour online) An example of LH coupling improved by putting the plasma close to the antenna; (a) I_P denotes the n_{e_av} line averaged density, $\langle RC \rangle$ the averaged reflection coefficient of LH, OV the oxygen impurity radiation; (b) geometries of the two selected discharges, LH antenna is located at $R = 2.37$ m, the distances between plasma and LH antenna are 7 cm and 5 cm respectively for #33335 and #33336.

An example of H-mode discharge using gas puffing is shown in Fig. 6. The D_2 gas was puffed at $t = 0.6$ s through a curved pipe installed on the poloidal plane of the outer wall about 1.4 m from the launcher. Then the neutral gas was allowed to diffuse to the nearby grill mouth, and be ionized there by the LH electric field. Since the line averaged density did not change enormously when the puffing started, the main plasma should be not affected by the gas injection. The reflection coefficient was about 5% during H-mode when the plasma–antenna distance was as short as 7 cm. The L–H transition occurred at $t = 2.9$ s, which is consistent with a sharp increase in global density and a drop in D_α emission below the L-mode level, and then the so-called 'big' ELMs were observed with a repetition frequency of 0.33 kHz, which is usually larger than that of other ELMs without gas injection, and a constant line-averaged density of 3.7×10^{19} m^{-3}, nearly twice as large as that in L phase. Subsequently, the discharge underwent a short ELMy-free period of about 0.2 s (see the enlarged part of the right central box in Fig. 6), during which the main plasma density increased again. After this quiescent H phase, the magnitude of the ELM burst became lower and the frequency became higher than that of previous types with a rather high plasma density (4.0×10^{19} m^{-3}), which is consistent with the characteristics of 'grassy' ELMs. Since the confinement of these ELMs stays almost as good as the original, we can infer that the electron density in SOL should decrease so that the LH coupling worsened as shown in the lower left box of Fig. 6. Finally the H phase terminated at $t = 6.6$ s, owing to the heating power being lower than the threshold power. In addition, no adverse effect on H-mode quality by gas puffing was observed.

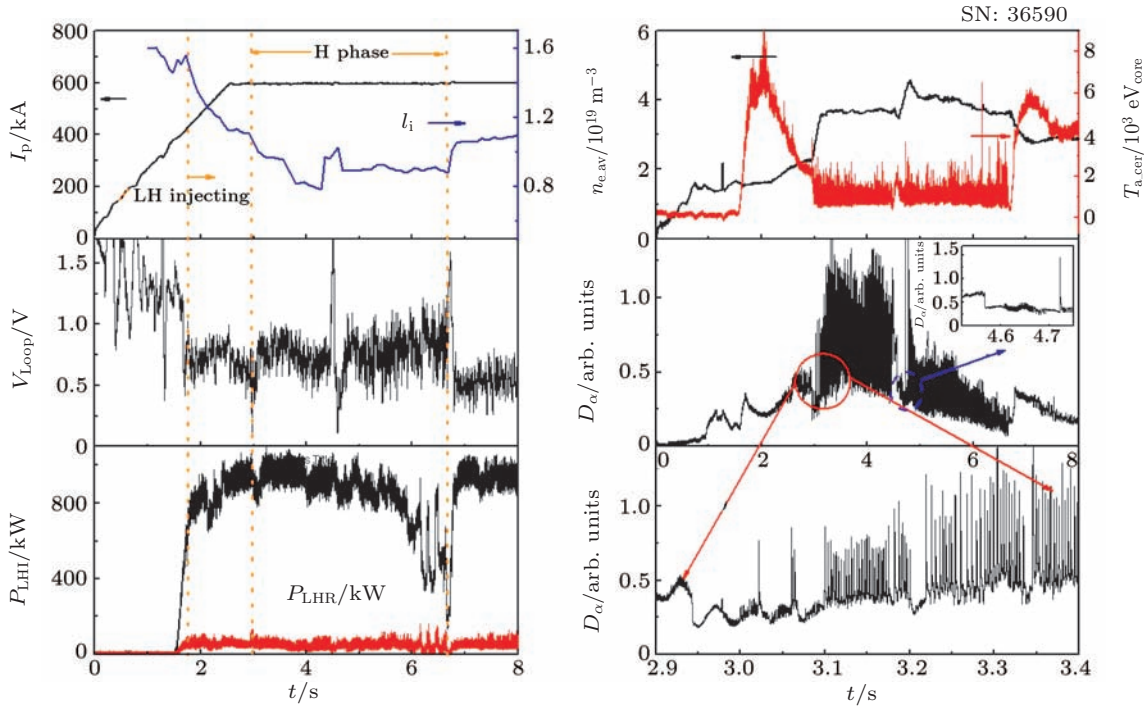


Fig. 6. (colour online) Time evolution of a 3.7-s H-mode discharge with LH injection (all the parameters are explained as mentioned above).

The LH was used at the current ramp-up stage to modify the current density profile $j(r)$ and to reduce the volt-second consumption. The LHCD properties are indirectly indicated by the evolution of internal inductance l_i: when LH injected, l_i gradually decreased from 1.5 to 1.1 until flat-top phase, indicating that $j(r)$ was successfully modified (note that, the value of 1.5 shows that the Ohmic current density profile is too peaked in the plasma core), and then during the flat-top phase before H-mode, l_i almost kept constant. During the big ELMs, it was seen that l_i continued to decrease which indicated the LH current shifted toward the more off-axis area than that in L phase, but its value became smaller inferred by the increase of

plasma surface loop voltage. Subsequently during the 2.0-s ELMy-free period, $l_{\rm i}$ suddenly began to increase instead of the preceding continuous drop. This is because the value of LH current decreased again due to the global density rising. Finally we could see that $l_{\rm i}$ fell after rising, which was definitely also related to the variation of plasma density. Moreover the result, the CD efficiency decreasing during the H-mode phase, is in good accordance with the trace of the electron–cyclotron emission (ECE) temperature, which is a measure of the LH coupling to fast electrons.[15] From the LHCD point of view, the parameter and the LH wave accessibility condition must be taken into account in EAST H-mode with low toroidal magnetic field. The accessibility condition $N_{\|}^{\rm acc}$ is given as[16]

$$N_{\|}^{\rm acc} = \omega_{\rm pe}/\omega_{\rm ce} + \sqrt{1 + (\omega_{\rm pe}/\omega_{\rm ce})^2 - (\omega_{\rm pi}/\omega)^2}, \quad (3)$$

where $\omega_{\rm pe}$ is the local electron plasma frequency, $\omega_{\rm ce}$ the local electron cyclotron, $\omega_{\rm pi}$ the local ion plasma frequency, and ω the wave frequency. The LH wave accessibility therefore depends on the local electron density and magnetic field. Waves with $N_{\|} > N_{\|}^{\rm acc}$ are accessible to the plasma centre, while waves with $N_{\|} < N_{\|}^{\rm acc}$ will be reflected from that layer. For EAST typical parameters: 1.3 T$\leq B_{\rm t} \leq$ 2 T, $N_{\|0} = 2.1$, density profile as shown in Fig. 2, the layer of mode conversion is located at about $r/a \sim 0.5$ where the local electron density is about 3.0×10^{19} m^{-3}. In other words, few rays can penetrate the plasma core and the power is mostly absorbed on the periphery. It should be noted that when using gas puffing to improve the LH coupling during H-mode, a fraction of the LH power would be parasitically absorbed by the excessive local electrons in front of the antenna. However such a drop in CD efficiency is indeed small in comparison with the effect of the loss of coupled power according to Ref. [11].

The modeling results of LH power deposition and current drive density by using the GENRAY code are shown in Fig. 7. GENRAY is a general ray tracing code for the calculation of electromagnetic wave propagation and absorption in the geometrical optics approximation.[17] The linear absorption of wave power along the ray trajectory is calculated as

$$P_{\rm abs} = P_0\left[1 - \exp(-2\int {\rm Im}(k){\rm d}l\right], \quad (4)$$

where P_0 is the wave power at launch point, l is the distance along the ray, and Im(k) is the imaginary part of wave vector. The integral is calculated along the ray trajectory. The code calculates the LH current density as $j = \eta P_{\rm abs}$ and CD efficiency η is determined by[17]

$$\eta = \frac{2}{(5+Z_{\rm eff})}\left(u^2 + \left(\frac{7}{4} + \frac{9}{4(3+Z_{\rm eff})}\right)\right), \quad (5)$$

where $u = c/N_{\|}v_{\rm th}$ is the resonance velocity normalized by electron thermal velocity $v_{\rm th}$. The input data such as $T_{\rm e}$ and $n_{\rm e}$ profiles are based on the H-mode discharge of #33067 as shown in Fig. 2. It is seen that LH current density profile during H phase is hollow with the peak located at about mid-radius while the value of LH current is $\sim$ 40 kA, almost half that in L phase. But experimental $I_{\rm LH}$ is uncertain.

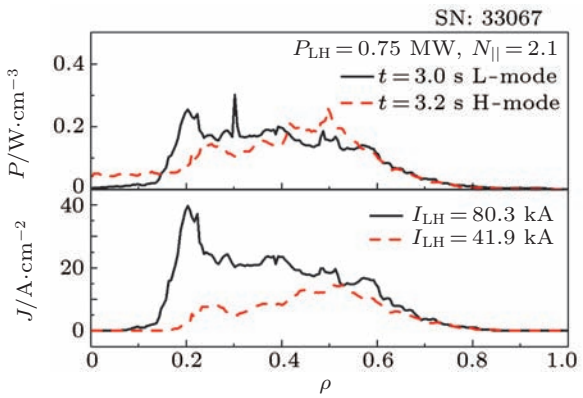


Fig. 7. (colour online) Modeling results of LH power deposition and current drive density profiles based on the experimental data of #33067.

4. Conclusions

The H-mode with LHCD alone is demonstrated in divertor discharges of EAST. These discharges exhibited many H-mode characteristics. The threshold power $P_{\rm th}$ for L–H transition follows the international tokamak scaling law. As a result of the SOL features of H-mode, great efforts are made to improve the LH coupling. The LHCD properties of CD efficiency and power deposition are indirectly indicated by some diagnostic measures, and well consistent with the numerical results.

Acknowledgement

The authors are grateful to the LHCD team for excellent support of EAST operations and diagnostics.

References

[1] Wagner F, Becker G, Behringer K, Campbell D, Eberhagen A, Engelhardt W, Fussmann G, Gehre O, Gernhardt J, Gierke G V, Haas G, Huang M, Karger F, Keilhacker M, Kluber O, Kornherr M, Lackner K, Lisitano G, Lister G G, Mayer H M, Meisel D, Muller E R, Murmann H, Niedermeyer H, Poschenrieder W, Rapp H, Bohr H, Schneider F, Siller G, Speth E, Stabler A, Steuer K H, Venus G, Vollmer O and Yu Z 1982 *Phys. Rev. Lett.* **49** 1408

[2] Kaye S M, Bell M, Bol K, Boyd D, Brau K, Buchenauer D, Budny R, Cavallo A, Couture P, Crowley T, Darrow D S, Eubank H, Fonck R J, Goldston R, Grek B, Jaehnig K P, Johnson D, Kaita R, Kugel H, Leblanc B, Manickam J, Manos D, Mansfield D, Mazzucato E, McCann R, McCune D, McGuire K, Mueller D, Murdock A, Okabayashi M, Okano K, Owens D K, Post D E, Reusch M, Schmidt G L, Sesnic S, Slusher R, Suckewer S, Surko C, Takahashi H, Tenney F, Towner H and Valley J 1984 *J. Nucl. Mater.* **121** 115

[3] Tubbing B J D, Jacquinot J J, Stork D and Tanga A 1989 *Nucl. Fusion***29** 1953

[4] Fielding S J, Ashall J D, Carolan P G, Colton A, Gates D, Hugill J, Morris A W, Valovic M, the COMPASS-D and ECRH Teams 1996 *Plasma Phys. Control Fusion* **38** 1091

[5] Keilhacker M, Becker G, Bernhardi K, Eberhagen A, ElShaer M, FuBmann G, Gehre O, Gernhardt J, Gierke G V, Glock E, Haas G, Karger F, Kissel S, Kluber O, Kornherr K, Lackner K, Lisitano G, Lister G G, Massig J, Mayer H M, McCormick K, Meisel D, Meservey E, Muller E R, Murmann H, Niedermeyer H, Poschenrieder W, Rapp H, Richter B, Rohr H, Ryter F, Schneider F, Siller S, Smeulders P, Soldner F, Speth E, Stabler A, Steinmetz K, Steuer K H, Szymanski Z, Venus G, Vollmer O and Wagner F 1984 *Plasma Phys. Control Fusion* **26** 49

[6] Biglari H, Diamond P H and Terry P W 1990 *Phys. Fluids* B **4** 1385

[7] Ding B J, Shan J F, Liu F K, Fang Y D, Wei W, Wu Z W, Chen Z Y, Xu H D, Wang M, Jiang M, Zhang G R, Huang F, Zhao Y P, Kuang G L and HT-7 Team 2006 *Chin. Phys.* **15** 2989

[8] JET Team 1991 *Proceedings of the Thirteenth International Conference on Plasma Physics and Controlled Nuclear Fusion Research* Seattle, USA IAEA-CN-53/A-IV-1/P261

[9] ITER Physics Expert Group on Confinement and Transport, ITER Physics Expert Group on Confinement Modelling and Database and ITER Physics Basis Editors 1999 *Nucl. Fusion* **39** 2175

[10] Doyle E J, Houlberg W A, Kamada Y, Mukhovatov V, Osborne T H, Polevoi A, Bateman G, Connor J W, Cordey J G, Fujita T, Garbet X, Hahm T S, Horton L D, Hubbard A E, Imbeaux F, Jenko F, Kinsey J E, Kishimoto Y, Li J, Luce T C, Martin Y, Ossipenko M, Parail V, Peeters A, Rhodes T L, Rice J E, Roach C M, Rozhansky V, Ryter F, Saibene G, Sartori R, Sips A C C, Snipes J A, Sugihara M, Synakowski E J, Takenaga H, Takizuka T, Thomsen K, Wade M R, Wilson H R, ITPA Transport Physics Topical Group, ITPA Confinement Database and Modelling Topical Group and ITPA Pedestal and Edge Topical Group 2007 *Nucl. Fusion* **47** S18

[11] Ekedahl A, Rantamäki K, Gonicheet M, Mailloux J, Petrzilka V, Alper B, Baranov Y, Basiuk V, Beaumont P, Corrigan G, Delpech L, Erents K, Granucci G, Hawkes N, Hobirk J, Imbeaux F, Joffrin E, Kirov K, Loarer T, McDonald D, Nave M F F, Nunes I, Ongena J, Parail V, Piccolo F, Rachlew E, Silva C, Sirinelli A, Stamp M, Zastrow K D and JET-EFDA Contributors 2009 *Plasma Phys. Control Fusion* **51** 044001

[12] Yan N, Xu G S, Zhang W, Chang J F, Ming T F, Ding S Y, Zhang W Y and Han X F 2010 *Plasma Sci. Technol.* **12** 401

[13] Ding B J, Li M H, Qin Y L, Li W K, Zhang L Z, Shan J F, Liu F K, Wang M, Meng L G, Xu H D, Wang D X, Jie Y X, Sun Y W, Shen B, Wang X M, Wu J H, Gao X, Zhang X D, Zhao Y P and HT-7 Team 2010 *Phys. Plasmas* **17** 022504

[14] Lu H W, Hu L Q, Zhou R J, Xu P, Zhong G Q, Lin S Y and Wang S F 2010 *Acta Phys. Sin.* **59** 7175 (in Chinese)

[15] Ushigusa K, Imai T, Ikeda Y, Sakamoto K, Söldner F X, Takase Y, Tsuji S, Shimizu K, Naito O, Uehara K, Akiba M, Araki M, Sato M, Yoshida Y, Nagashima K, Kusama Y, Kubo H, Nemoto M and Tobita K 1989 *Nucl. Fusion* **29** 265

[16] Stix T H 1962 *The Theory of Plasma Waves* (New York: McGraw-Hill)

[17] Smirnov A P and Harvey R W 2003 *The GENRAY Ray Tracing Code Technical Report* CompX-2000-01, version 2